JVI Journals.ASM.org

Negative Regulation of RIG-I-Mediated Innate Antiviral Signaling by SEC14L1

Meng-Tong Li,[a] Wei Di,[b] Hao Xu,[a] Yong-Kang Yang,[a] Hai-Wei Chen,[a] Fei-Xiong Zhang,[b] Zhong-He Zhai,[a] Dan-Ying Chen[a]

The Key Laboratory of Cell Proliferation and Differentiation of the Ministry of Education, College of Life Sciences, Peking University, Beijing, China[a]; College of Life Sciences, Capital Normal University, Beijing, China[b]

Retinoic acid-inducible gene I (RIG-I) is a key sensor for recognizing nucleic acids derived from RNA viruses and triggers beta interferon (IFN-β) production. Because of its important role in antiviral innate immunity, the activity of RIG-I must be tightly controlled. Here, we used yeast two-hybrid screening to identify a SEC14 family member, SEC14L1, as a RIG-I-associated negative regulator. Transfected SEC14L1 interacted with RIG-I, and endogenous SEC14L1 associated with RIG-I in a viral infection-inducible manner. Overexpression of SEC14L1 inhibited transcriptional activity of the IFN-β promoter induced by RIG-I but not TANK-binding kinase 1 (TBK1) and interferon regulatory factor 3 (IRF3). Knockdown of endogenous SEC14L1 in both HEK293T cells and HT1080 cells potentiated RIG-I and Sendai virus-triggered IFN-β production as well as attenuated the replication of Newcastle disease virus. SEC14L1 interacted with the N-terminal domain of RIG-I (RIG-I caspase activation and recruitment domain [RIG-I-CARD]) and competed with VISA/MAVS/IPS-1/Cardif for RIG-I-CARD binding. Domain mapping further indicated that the PRELI-MSF1 and CRAL-TRIO domains but not the GOLD domain of SEC14L1 are required for interaction and inhibitory function. These findings suggest that SEC14L1 functions as a novel negative regulator of RIG-I-mediated antiviral signaling by preventing RIG-I interaction with the downstream effector.

Cellular antiviral innate immunity involves host pattern recognition receptors (PRRs), which recognize invading viruses and initiate a series of signaling events leading to the production of type I interferons (IFNs) and proinflammatory cytokines. Four subfamilies of PRRs have been identified: membrane-bound Toll-like receptors, C-type lectin receptors, and cytoplasmic proteins such as NOD-like receptors and retinoic acid-inducible gene I (RIG-I)-like receptors (RLRs) (1).

Among the PRRs, at least two distinct families can recognize viral RNA (2). One is the Toll-like receptors; for example, Toll-like receptor 3 (TLR3), TLR7, and TLR8 recognize double-stranded RNA (dsRNA) or single-stranded RNA (ssRNA) at the membrane of endosomes. Another family is RLRs such as RIG-I (also called DDX58), MDA5 (melanoma differentiation-associated gene 5), and LGP2 (laboratory of genetics and physiology 2). They are localized in the cytoplasm and recognize the genomic RNA of dsRNA viruses and dsRNA generated as the replication intermediate of ssRNA viruses (3–7). The expression of RLRs is greatly enhanced in response to type I interferon stimulation or viral infection.

All three members share a highly conserved domain structure including a DExD-box RNA helicase/ATPase domain and a C-terminal regulatory domain, also termed the repressor domain (RD) (8, 9). RIG-I and MDA5, but not LGP2, contain two N-terminal tandem caspase activation and recruitment domains (CARDs), which mediate signaling to downstream adaptor proteins. Structural studies of individual RIG-I domains have provided some insight into the atomic mechanism of recognition of viral dsRNA and the activation of RIG-I (10). Current models suggest that in the absence of viral RNA, the basal activity of RIG-I is controlled by autoinhibition (11). The binding of viral RNA, which contains 5′-triphosphate and certain duplex structures, to the C-terminal regulatory and helicase domains of RIG-I induces an ATP-dependent conformational change, which exposes the CARDs (12, 13).

Protein modifications also play important roles in regulating the activity of RIG-I and signal transduction. The exposed CARDs recruit the ubiquitin E3 ligase TRIM25 to catalyze the synthesis of Lys63 (K63) polyubiquitin chains (14, 15). These ubiquitin chains bind to and activate CARDs and induce the oligomerization of RIG-I *in vitro* and in virus-infected cells. It has been reported that REUL/Riplet, an E3 ubiquitin ligase, is also involved in this process (16–18). Oligomerized RIG-I molecules are recruited to mitochondria, where the released CARDs interact with the CARD of the signaling adaptor VISA/MAVS/IPS-1/Cardif (19–22). This interaction promotes the prion-like aggregation of VISA on the mitochondrial membrane and propagates antiviral signaling (23). VISA then activates the cytosolic protein kinases IκB kinase (IKK) and TANK-binding kinase 1 (TBK1). TBK1 phosphorylates the transcription factor interferon regulatory factor 3 (IRF3), which causes IRF3 to dimerize and translocate to the nucleus, where IRF3 and other transcriptional factors function together to induce the expression of type I interferons and other antiviral molecules.

In the present study, we identified a SEC14 family member, SEC14L1, as a RIG-I-associated protein through yeast two-hybrid screening. SEC14L1 is reported to be a phospholipid transfer protein. It interacts with the vesicular acetylcholine transporter, which suggests a possible involvement in regulating cholinergic neurotransmission (24). Our data demonstrated that SEC14L1 also plays an important role in innate immunity. Overexpressed SEC14L1 interacted with RIG-I and inhibited RIG-I-mediated

Received 20 April 2013 **Accepted** 26 June 2013

Published ahead of print 10 July 2013

Address correspondence to Fei-Xiong Zhang, fxzhang@hotmail.com, or Dan-Ying Chen, dychen@pku.edu.cn.

M.-T.L. and W.D. contributed equally to this work.

doi:10.1128/JVI.01073-13

downstream signaling and antiviral activity. Knockdown of endogenous SEC14L1 potentiated Sendai virus (SeV)-triggered beta interferon (IFN-β) production and viral replication. SEC14L1 interacted only with the RIG-I-CARDs and inhibited the formation of the RIG-I-CARD–VISA complex. These finding suggest that SEC14L1 inhibits RIG-I-mediated innate antiviral signaling.

MATERIALS AND METHODS

Reagents and cell lines. Mouse or rabbit antibodies against Flag and hemagglutinin (HA) epitopes (Sigma-Aldrich, USA), IRDye800-conjugated anti-mouse antibody (Rockland Immunochemicals, USA), mouse monoclonal antibody to RIG-I (Alexis Biochemicals, Switzerland), rabbit polyclonal antibodies against IRF3 (SC-9082), goat polyclonal antibodies against SEC14L1 (SC-1654444), mouse anti-VISA antibody and SeV (Hong-Bing Shu, Wuhan University, China), Newcastle disease virus (NDV)-enhanced green fluorescent protein (eGFP) (Cheng Wang, Institute of Biochemistry and Cell Biology, Shanghai, China), and the 2fTGH cell line (Zheng-Fan Jiang, Peking University, China) were obtained from the indicated sources. HEK293T, HT1080, and HeLa cells were grown in Dulbecco's modified Eagle's medium (DMEM) supplemented with 10% fetal bovine serum.

Yeast two-hybrid screens. The human fetal kidney cDNA library (Clontech, USA) was screened with full-length RIG-I as bait, according to protocols recommended by the manufacturer.

Constructs. Mammalian expression plasmids for Flag- or HA-tagged SEC14L1, RIG-I, REUL, TRIM25, and their deletion mutants were constructed by standard molecular biology techniques. Mammalian expression plasmids for Flag-VISA, -TBK1, -IRF3, and -IRF3-5D and interferon-stimulated release element (ISRE) and IFN-β promoter luciferase reporter plasmids were kindly provided by Hong-Bing Shu (Wuhan University, China).

Transfection and luciferase assays. HEK293T cells ($\sim 1 \times 10^5$) were seeded onto 24-well dishes and transfected the next day by standard calcium phosphate precipitation. To normalize for transfection efficiency, 100 ng of the pRL-TK (*Renilla* luciferase) reporter plasmid was added to each transfection mixture. Luciferase assays were performed with a dual-specific luciferase assay kit (Promega, USA). Firefly luciferase activity was normalized to the *Renilla* luciferase activity. All reporter assays were repeated at least three times. Data shown are average values ± standard deviations (SD) from three independent experiments.

Immunofluorescent staining. Cells were fixed in ice-cold methanol for 10 min at −20°C, rehydrated three times with phosphate-buffered saline (PBS), and blocked in 5% bovine serum albumin–PBS for 10 min. The cells were stained with primary antibody in blocking buffer for 1 h at 37°C, rinsed with PBS, and stained again with fluorescein isothiocyanate (FITC)-labeled rabbit anti-mouse IgG or Texas Red-labeled goat anti-rabbit IgG (Kirkegaard & Perry Laboratories) for 1 h at 37°C. The cells were then rinsed with PBS containing 4′,6-diamidino-2-phenylindole (DAPI) and mounted. The cells were observed under an Olympus BX51 immunofluorescence microscope using a 100× plan objective.

Coimmunoprecipitation and Western blot analysis. For transient-transfection and immunoprecipitation experiments, HEK293T cells ($\sim 2 \times 10^5$) were transfected with the indicated plasmids for 20 h. The transfected cells were lysed in 0.5 ml of lysis buffer (20 mM Tris [pH 7.5], 150 mM NaCl, 1% Triton X-100, 1 mM EDTA, 10 mg/ml aprotinin, 10 mg/ml leupeptin, and 1 mM phenylmethylsulfonyl fluoride). For each immunoprecipitation, a 0.4-ml aliquot of lysate was incubated with 0.5 μg of the indicated antibody and 25 μl of a 1:1 slurry of protein A-Sepharose (GE Healthcare, USA) for 2 h. The Sepharose beads were washed three times with 1 ml of lysis buffer. The precipitates were analyzed by Western blotting with the indicated antibodies and visualized by incubation with IRDye800-conjugated secondary antibodies (diluted 1:10,000), using an Odyssey infrared imaging system (Licor Inc., Germany).

Native PAGE. A native PAGE gel (8%) was prerun for 30 min at 40 mA with native running buffer (25 mM Tris and 192 mM glycine [pH 8.4]) and with 0.5% deoxycholate in the cathode chamber. Samples were prepared in native sample buffer (62.5 mM Tris-HCl [pH 6.8], 40% glycerol, and 0.01% bromophenol blue).

Semiquantitative RT-PCR. Total RNA was isolated from cells by using TRIzol reagent (Transgen Biotech Co., Beijing, China) and subjected to semiquantitative reverse transcription-PCR (RT-PCR) analysis to measure the expression levels of IFN-β, SEC14L1, β-actin, and RIG-I. The gene-specific primer sequences were 5′-CCAACAAGTGTCTCCTCCA A-3′ for the IFN-β sense primer and 5′-ATAGTCTCATTCCAGCCAG T-3′ for the IFN-β antisense primer, 5′-CTGCTACACCGTTCACCCTG A-3′ for the SEC14L1 sense primer and 5′-GGGGCACAAAGGTTATGC CTT-3′ for the SEC14L1 antisense primer, 5′-ACGTGGACATCCGCAA AGAC-3′ for the β-actin sense primer and 5′-CAAGAAAGGGTGTAAC GCAACTA-3′ for the β-actin antisense primer, and 5′-GGGCTGACTG CCTCGGTTGG-3′ for the RIG-I sense primer and 5′-TGTGCCGGGAG GGTCATTCCT-3′ for the RIG-I antisense primer.

RNAi experiments. Double-stranded oligonucleotides corresponding to the target sequences were cloned into the pSuper.retro RNA interference (RNAi) plasmid (Oligoengine, USA). In this study, the target sequences for human SEC14L1 cDNA were 1# (5′-AAAGCCAGAGAGAT CATGTGT-3′), 2# (5′-AAAGCAGCATCAGGTAGACTA-3′), 3# (5′-AA AGAGATTATTCCAGA-3′), and 4# (5′-AACAATGTGCAGCTCATAG AC-3′).

Plasmids encoding lentiviruses expressing short hairpin RNAs (shRNAs) were obtained from the library of the RNAi Consortium (Sigma-Aldrich). Plasmids were purified and then transfected into HEK293T cells with a three-plasmid system to produce lentivirus. The following shRNAs were produced: SEC14L1sh1# (target sequence CC GGGCAGGAGTTGATTATGTTTATCTCGAGATAAACATAATCAAC TCCTGCTTTTTG), SEC14L1sh2# (target sequence CCGGGTTCCTCA TTTATGCAGGAAACTCGAGTTTCCTGCATAAATGAGGAACTTTT TG), and the control hairpin GFPsh (a scrambled sequence against GFP). HT1080 cells were plated onto a 6-well plate at $\sim 5 \times 10^5$ cells per well with 2 ml complete medium. One milliliter of the indicated lentivirus was added. The plates were incubated for 48 h, and the cells were selected with 1 mg/ml puromycin. Cells were collected for analysis 72 h after selection.

Virus infection and flow cytometry analyses. The percentage of cells infected with NDV-eGFP was determined based on GFP expression. HEK293T cells were transfected with plasmids 24 h before NDV-eGFP infection. Cells were then analyzed on a flow cytometer (BD FACSCalibur). Cell population analysis was done by using Cell Quest.

Type I IFN bioassays. Type I IFN activity was measured with a 2fTGH cell line stably transfected with an interferon-sensitive (ISRE) luciferase construct. The supernatants collected from HT1080 cells with stimuli were added to the 2fTGH cell line. After 4 h, 2fTGH cells were lysed, and firefly luciferase activity was measured. HT1080 cells were stained with 3-(4,5-dimethyl-2-thiazolyl)-2,5-diphenyl-2H-tetrazolium bromide (MTT) to assess viability after the stated time interval.

RESULTS

SEC14L1 interacts with RIG-I. It is well known that RIG-I is an important cytosolic sensor for the antiviral innate immune response. To identify proteins that interact with RIG-I and regulate its signaling, we performed a yeast two-hybrid screen of the human fetal kidney cDNA library using full-length RIG-I as bait. We screened 3×10^6 independent clones, and 1 of 19 positive clones encoded the C-terminal region of SEC14L1 (amino acids [aa] 287 to 715). SEC14L1 is a poorly characterized member of the SEC14 family in mammals with the potential to control the local phospholipid content in membranes (25–27). Because SEC14L1 interacted with RIG-I in the yeast two-hybrid system, we determined whether this interaction also occurs in mammalian cells. We transfected HEK293T cells with expression plasmids for hemagglutinin (HA)-tagged SEC14L1 and Flag-tagged RIG-I and per-

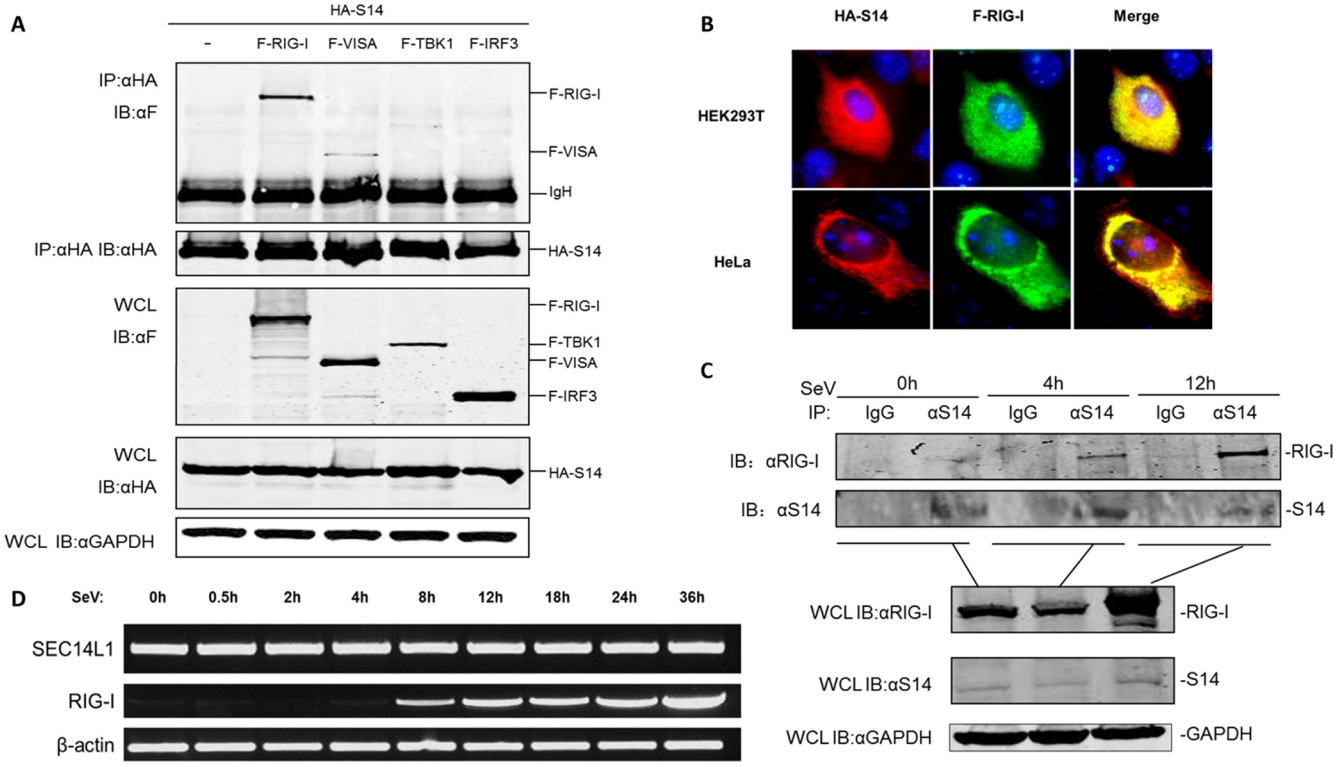

FIG 1 SEC14L1 associates with RIG-I. (A) SEC14L1 interacted with RIG-I but not TBK1 and IRF3. HEK293T cells (1×10^6) were transfected with HA-SEC14L1 (HA-S14) alone or together with Flag–RIG-I (F-RIG-I), Flag-VISA, Flag-TBK1, or Flag-IRF3 plasmids (6 μg each). Cell lysates were immunoprecipitated (IP) with anti-HA (αHA). The immunoprecipitates were analyzed by Western blotting (immunoblotting [IB]) with anti-Flag (αF). Whole-cell lysates (WCL) were analyzed by Western blotting with anti-HA, anti-Flag, and anti-glyceraldehyde-3-phosphate dehydrogenase (GAPDH). (B) HEK293T or HeLa cells were transfected with HA-SEC14L1 and Flag–RIG-I. Immunofluorescent staining was performed with anti-HA (red) and anti-Flag (green). (Top) HEK293T cells were transfected with HA-SEC14L1 (stained red) and Flag–RIG-I (stained green). (Bottom) HeLa cells were transfected and stained as in the top panels. The experiments were repeated twice, and similar results were obtained. (C) Endogenous interaction of SEC14L1 and RIG-I. HEK293T cells were treated with SeV for 4 h and 12 h or left untreated (−). Cell lysates were immunoprecipitated with goat anti-SEC14L1 antiserum or control IgG. The immunoprecipitates were analyzed by Western blotting with mouse anti-RIG-I antibody. The expression levels of the endogenous proteins were analyzed by Western blotting with anti-RIG-I and anti-SEC14L1 antibodies. (D) mRNA level of SEC14L1 after SeV infection. HEK293T cells (2×10^5) infected with SeV were treated for the indicated times. Total RNA was isolated, and RT-PCR was performed by using the indicated primers.

formed coimmunoprecipitation experiments. The results showed that SEC14L1 associated with RIG-I in mammalian cells (Fig. 1A), and this interaction was relatively specific because in the same experiment, SEC14L1 had a weak interaction with the adaptor protein VISA but not with TBK1 and IRF3, which are downstream signaling proteins of RIG-I (Fig. 1A).

SEC14L1 has been reported to be localized predominantly in the cytosol, with little or none in defined organelles (24). We found that SEC14L1 colocalized with RIG-I in cotransfected HEK293T and HeLa cells. Double-immunofluorescent staining showed that overexpressed SEC14L1 had a similar distribution pattern and overlapped RIG-I (Fig. 1B). These observations substantiated the outcome of the yeast two-hybrid assay and confirmed a direct interaction between RIG-I and SEC14L1.

We further confirmed the physiological association of SEC14L1 with RIG-I and the effects of viral infection on the interaction by performing coimmunoprecipitation with anti-SEC14L1 antibody in HEK293T cells with or without SeV infection. The results showed that endogenous RIG-I interacted extremely weakly with endogenous SEC14L1 in the absence of SeV infection. However, a distinct interaction appeared 4 h after SeV infection, and the interaction was markedly enhanced with time due to the inducible expression of RIG-I (Fig. 1C). We also performed a time course experiment to detect whether SEC14L1 expression is induced by virus infection. RT-PCR results showed that the mRNA level of SEC14L1 had not changed after SeV infection in HEK293T cells (Fig. 1D). These results suggested that SEC14L1 associates with RIG-I in a viral infection-inducible manner.

SEC14L1 inhibits RIG-I-mediated signaling. Because SEC14L1 associated with RIG-I, we then determined whether SEC14L1 is involved in the regulation of RIG-I signaling. In reporter assays, overexpression of SEC14L1 alone had no apparent effects on the activation of the interferon-stimulated release element (ISRE) and IFN-β promoters. However, in cotransfection experiments in HEK293T cells, the induction of IFN-β and ISRE promoter activity by RIG-I and the N-terminal CARD of RIG-I (RIG-I-CARD), which potently activate downstream signaling, was dose-dependently inhibited by SEC14L1 (Fig. 2A and B). We further tested whether SEC14L1 targets downstream components in the RIG-I signaling pathway. We found that SEC14L1 partly inhibited the VISA-induced IFN-β and ISRE promoters but not TBK1 and constitutively activated IRF3 (S396D, S398D, S402D, T404D, and S405D, referred to as IRF3-5D) (28) (Fig. 2C). In RT-PCR experiments, cotransfection of SEC14L1 apparently reduced the mRNA

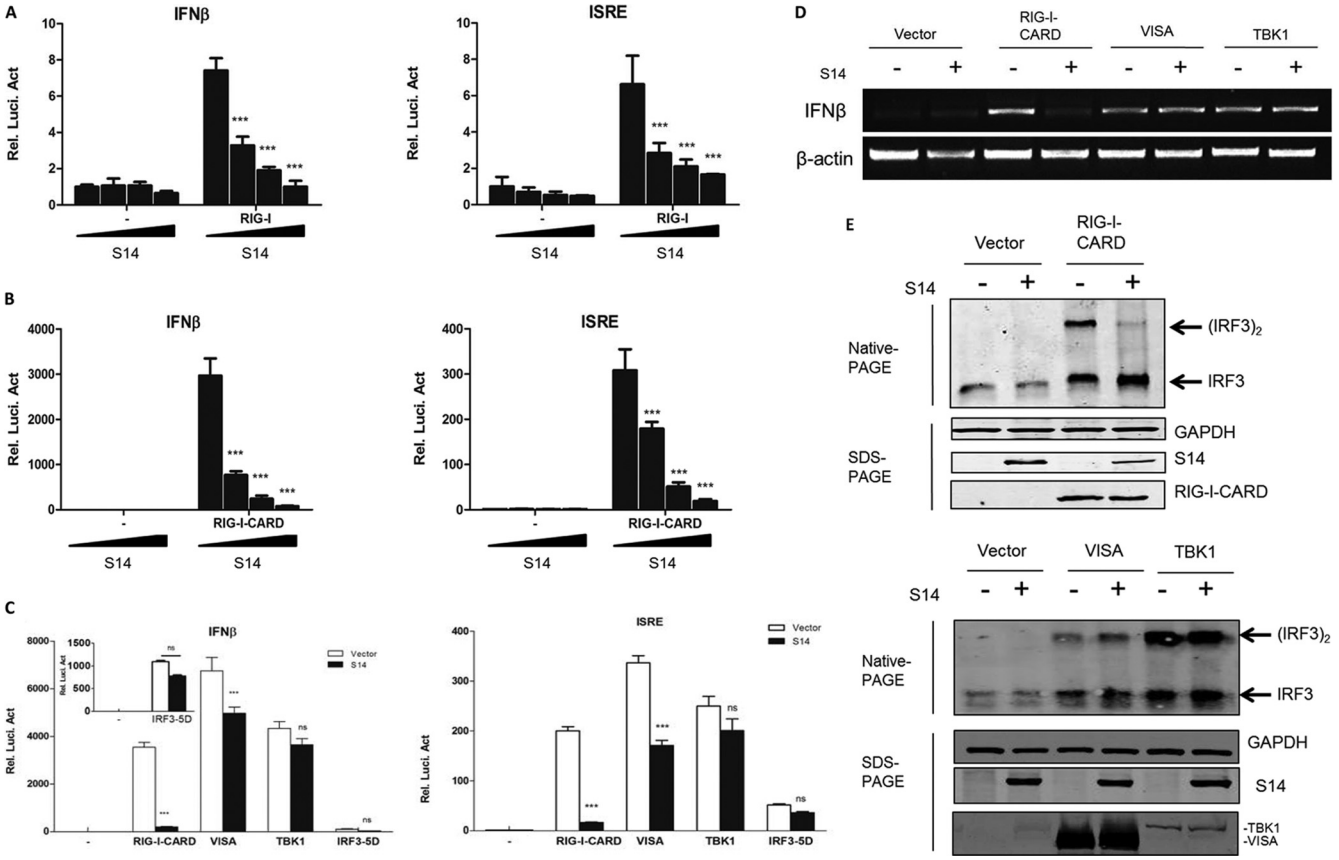

FIG 2 SEC14L1 inhibits RIG-I-mediated signaling. (A and B) SEC14L1 inhibits RIG-I (A)- and RIG-I-CARD (B)-mediated activation of ISRE and IFN-β promoters in a dose-dependent manner. Gene induction in HEK293T cells transfected with luciferase reporter constructs driven by promoters of genes encoding the IFN-β or interferon-stimulated response element (ISRE) plus 100 ng of various plasmids (horizontal axes) and 0, 100, 200, or 400 ng (wedges) of SEC14L1, assessed as luciferase activity after 24 h, is shown; results are presented relative to the luciferase activity in control cells (transfected with the luciferase reporter and empty vector). (C) SEC14L1 has effects on the activation of the IFN-β and ISRE promoters mediated by RIG-I-CARD and VISA but not by TBK1 and IRF3-5D. HEK293T cells (1×10^5) were transfected with the indicated reporter plasmid (100 ng) and expression plasmids (400 ng of each). Reporter assays were performed 20 h after transfection. (D) SEC14L1 inhibits RIG-I- but not VISA- and TBK1-mediated IFN-β expression. HEK293T cells (2×10^5) were transfected with the indicated plasmids. Twenty-four hours after transfection, total RNA was isolated, and RT-PCR was performed by using the indicated primers. (E) SEC14L1 inhibits RIG-I-CARD- but not VISA- and TBK1-mediated IRF3 dimerization. HEK293T cells (2×10^5) were transfected with the indicated plasmids. Twenty-four hours after transfection, cell lysates were separated by native PAGE (top) or SDS-PAGE (bottom) and analyzed by immunoblotting with the indicated antibodies. For panels A to C, data show means ± SD of triplicate values and are from three independent experiments. ***, $P < 0.001$; ns, not significant.

level of IFN-β induced by RIG-I-CARD but not VISA and TBK1 (Fig. 2D). Biochemically, SEC14L1 selectively inhibited the dimerization of IRF3 induced by RIG-I-CARD but not VISA and TBK1 (Fig. 2E), which is a hallmark of IRF3 activation (29). Taken together, these results suggested that SEC14L1 specifically inhibits RIG-I but not IFN-β promoter activation mediated by downstream effectors.

Knockdown of SEC14L1 potentiates RIG-I signaling. To validate the repressive effect of endogenous SEC14L1 on RIG-I, we used two systems to knock down endogenous SEC14L1 in different cell types. First, we constructed four SEC14L1-RNAi pSuper plasmids targeting different sites in human SEC14L1 mRNA. Transient transfection in HEK293T cells and Western blot analysis showed that one of these RNAi plasmids (4#) markedly inhibited the expression of transfected SEC14L1 (Fig. 3A). SEC14L1 suppression correlated with the activation of the IFN-β and ISRE promoters potentiated by RIG-I and RIG-I-CARD but not that induced by VISA, TBK1, and IRF3-5D, compared with the control RNAi plasmids 1#, 2#, and 3# (Fig. 3B). Consistent with this, RT-PCR showed that transfection with RNAi plasmid 4# enhanced the expression of endogenous IFN-β induced by RIG-I and RIG-I-CARD (Fig. 3C). These results further confirmed the conclusion that SEC14L1 specifically inhibits RIG-I.

SEC14L1 plays a role in regulating the cellular antiviral response mediated by RIG-I. It is known that SeV and Newcastle disease virus (NDV) infections trigger IFN-β production in a RIG-I-dependent manner. Therefore, we further determined whether SEC14L1 played roles in the virus-triggered IFN signaling mediated by RIG-I. In reporter gene assays, overexpression of SEC14L1 dose-dependently inhibited the activation of the IFN-β and ISRE promoters induced by SeV infection (Fig. 4A). Consistently, RT-PCR showed that transfection with SEC14L1 inhibited the SeV-induced expression of endogenous IFN-β (Fig. 4B) and the dimerization of IRF3 (Fig. 4C).

We also used lentivirus-delivered short hairpin RNAs (shRNAs) to knock down endogenous SEC14L1 expression in HT1080 cells. We obtained stable HT1080 cell lines with GFPsh, SEC14L1sh1#, and SEC14L1sh2# by selection with puromycin. As shown by the

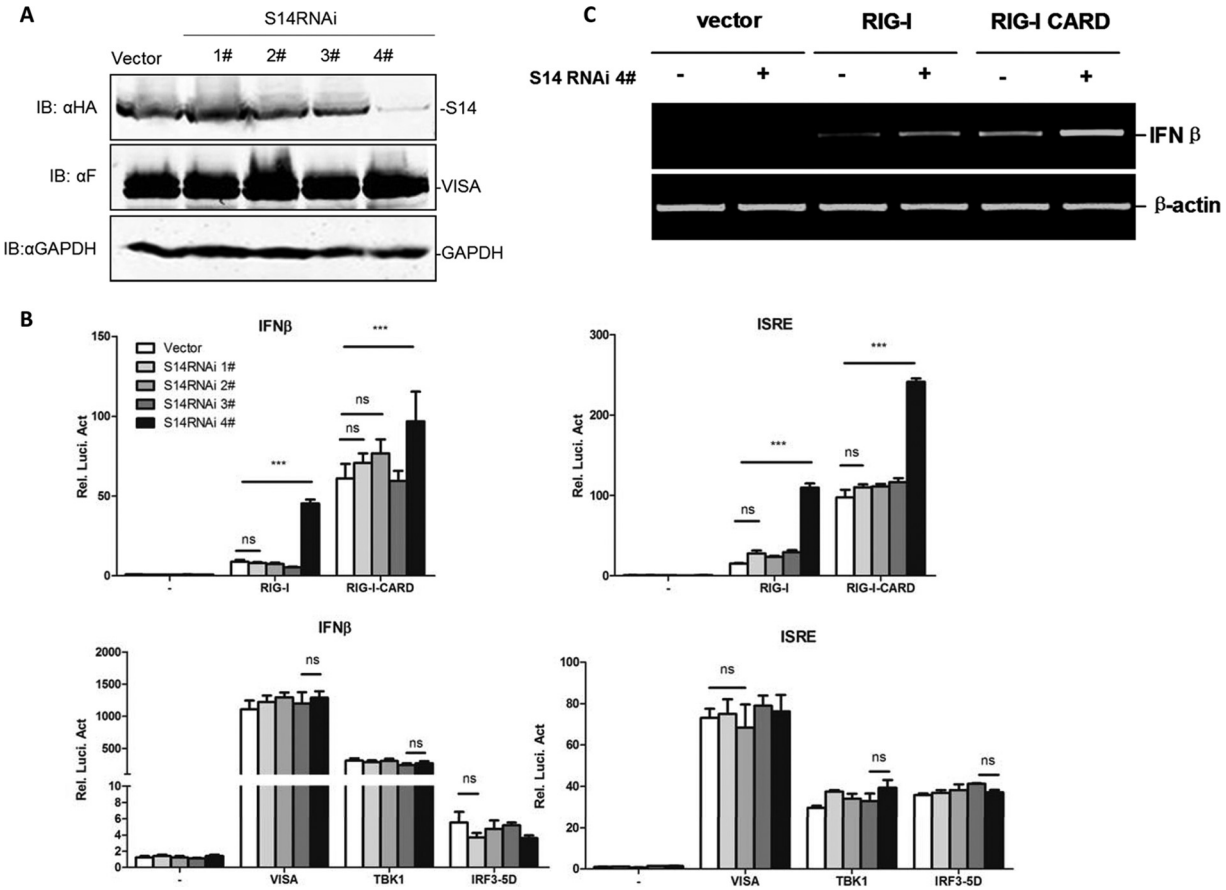

FIG 3 Knockdown of SEC14L1 potentiates RIG-I signaling. (A) Effects of SEC14L1 pSuper RNAi plasmids on the expression of transfected SEC14L1. HEK293T cells (2×10^5) were transfected with expression plasmids for HA-SEC14L1, as well as Flag-VISA as a control (0.5 μg each), and the indicated RNAi plasmids (1 g). At 48 h after transfection, cell lysates were analyzed by Western blotting with anti-Flag, anti-HA, and anti-GAPDH antibodies. (B) SEC14L1 RNAi plasmid potentiates the activation of the IFN-β and ISRE promoters induced by RIG-I and RIG-I-CARD but not by VISA, TBK1, and IRF3-5D. HEK293T cells (2×10^5) were transfected with the indicated reporter plasmid (100 ng), the pRL-TK *Renilla* luciferase plasmid (100 ng), and the indicated SEC14L1 RNAi plasmid (500 ng). At 48 h after transfection, luciferase assays were performed. (C) SEC14L1 RNAi enhances RIG-I- and RIG-I-CARD-mediated gene expression. HEK293T cells (2×10^5) were transfected with the indicated plasmids. Forty-eight hours after transfection, total RNA was isolated, and RT-PCR was performed by using the indicated primers.

mRNA levels, one shRNA (SEC14Lsh1#) inhibited SEC14L1 expression compared to the shRNA control (GFPsh) (Fig. 4D). SEC14L1 knockdown resulted in a boosted expression of endogenous IFN-β in RT-PCR experiments at 12 h after SeV infection (Fig. 4E). Consistently, enhanced dimerization of IRF3 occurred at 6 h after SeV stimulation and was most evident at 12 h after stimulation in SEC14L1 knockdown cells (Fig. 4F). In type I IFN bioassays, we found that SEC14L1 depletion prompted an increase in IFN-β production in HT1080 cells at 6 h after SeV infection and a significant increase after 6 h of SeV stimulation. Also, SeV-triggered IFN-β production in knockdown SEC14L1 cells occurred much earlier and lasted longer than in shRNA controls (Fig. 4G).

Next, we determined whether endogenous SEC14L1 plays an inhibitory role in the cellular antiviral response. Upon infection by NDV-enhanced green fluorescent protein (NDV-eGFP), overexpressed SEC14L1 enhanced NDV-eGFP replication in HEK293T cells. We further found that overexpression of SEC14L1 obviously reduced the inhibitory effect on viral replication mediated by RIG-I-CARD (Fig. 4H). Consistently, SEC14L1 RNAi rendered cells remarkably resistant to viral replication and reduced the numbers of NDV-eGFP-positive cells. Depletion of SEC14L1 also dramatically reduced viral infection mediated by RIG-I (Fig. 4H). By flow cytometry analysis, overexpressed SEC14L1 enhanced the percentage of NDV-eGFP-positive cells mediated by RIG-I-CARD. SEC14L1 RNAi made cells resistant to viral infection, and NDV-eGFP infectivity was reduced from 21% to 12%, about a 1.75-times reduction mediated by RIG-I-CARD (Fig. 4I). Collectively, these data suggested that SEC14L1 is a physiological suppressor of the RIG-I-mediated cellular antiviral response.

SEC14L1 competes with VISA for RIG-I-CARD binding. In order to determine which domain of RIG-I is responsible for the interaction, we cotransfected full-length RIG-I (RIG-I-FL) (residues 1 to 925), RIG-I-CARD (residues 1 to 218), RIG-I-helicase (residues 219 to 791), RIG-I-RD (residues 792 to 925), and RIG-I-ΔCARD (residues 220 to 925) with SEC14L1 and performed coimmunoprecipitation assays. We found that SEC14L1 interacted only with the RIG-I-CARD independently as well as RIG-I-FL, whereas it did not interact with CARD deletion mutations (Fig. 5A). It was shown that RIG-I-CARD interacts with VISA through a CARD-CARD interaction. The finding that SEC14L1

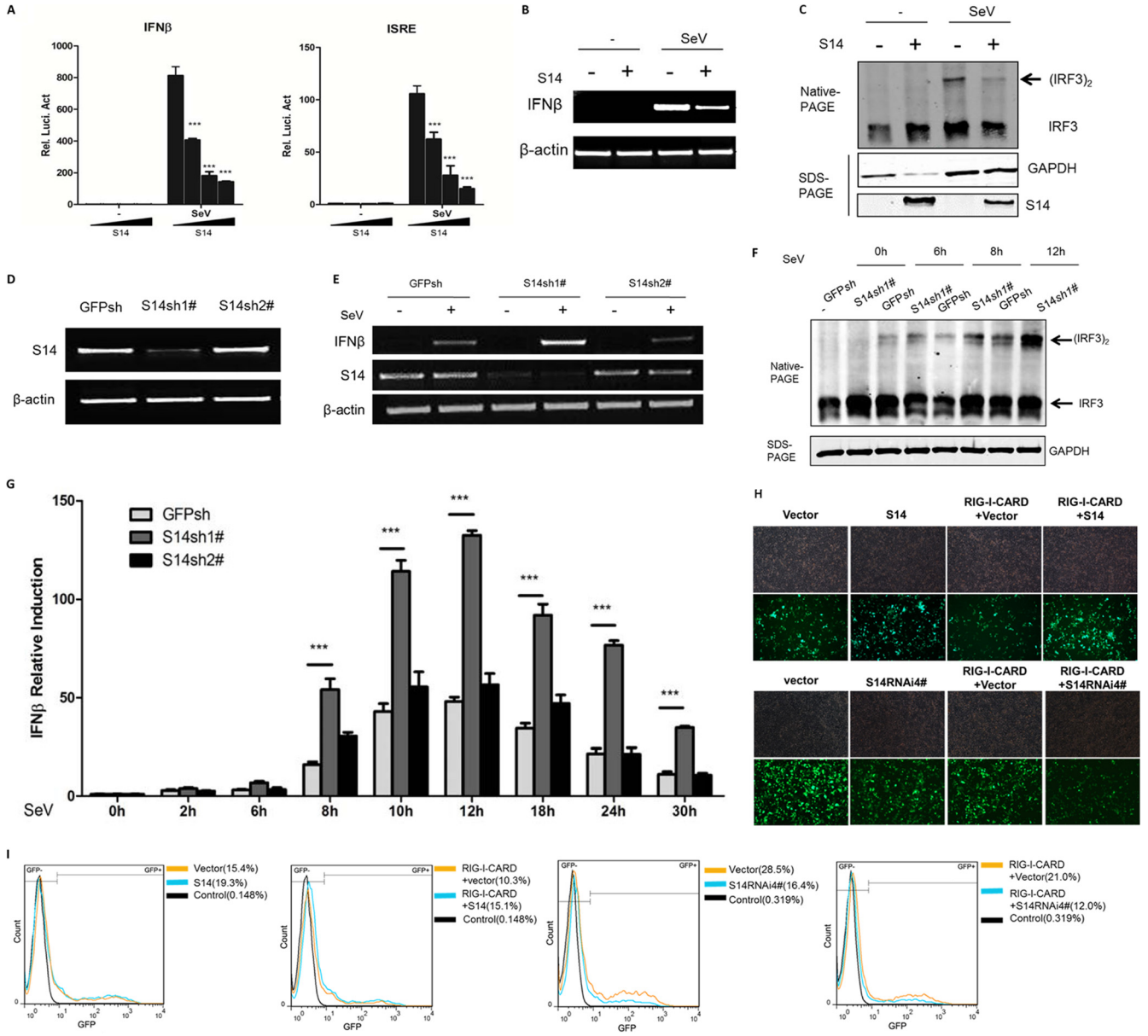

FIG 4 SEC14L1 plays a role in regulation of the RIG-I-mediated cellular antiviral response. (A) SEC14L1 suppresses SeV-induced activation of the ISRE and IFN-β promoters in a dose-dependent manner. Gene induction was performed with HEK293T cells transfected for 12 h with the indicated reporter plasmid, and they were then infected for 18 h with SeV or left uninfected, followed by analysis as described in the legend of Fig. 2A. (B) SEC14L1 inhibits virus-induced IFN-β expression. HEK293T cells (2×10^5) were transfected with the indicated plasmids for 24 h and then infected for 12 h with SeV. Total RNA was isolated, and RT-PCR was performed by using the indicated primers. (C) SEC14L1 inhibits SeV-triggered IRF3 dimerization. HEK293T cells (2×10^5) were transfected with the indicated plasmids for 18 h and then infected with SeV for 12 h. Cell lysates were separated by native PAGE (top) or SDS-PAGE (bottom) and analyzed by immunoblotting with the indicated antibodies. (D) Effect of shSEC14L1 plasmids on endogenous SEC14L1. RT-PCR was performed after infection with three lentiviruses encoding an shRNA control (GFPsh) and two shRNAs targeting SEC14L1 (S14sh#1 and S14sh#2) with the indicated primers in HT1080 human fibrosarcoma cells. (E) Knockdown of SEC14L1 enhances SeV-induced IFN-β expression. HT1080 cells were infected with SeV for 12 h, total RNA was isolated, and RT-PCR was performed by using the indicated primers. (F) Knockdown of SEC14L1 enhances SeV-triggered IRF3 dimerization. HT1080 cells were infected with SeV for the indicated times. Cell lysates were separated by native PAGE (top) or SDS-PAGE (bottom) and analyzed by immunoblotting with the indicated antibodies. (G) SEC14L1 knockdown in HT1080 cells potentiates SeV-induced IFN-β production. HT1080 cells infected with SeV were treated for the indicated times (horizontal axes). A bioassay of type I interferon in supernatants of HT1080 cells was performed, and results are presented relative to the results of the bioassay with untreated control cells. Data show means ± SD ($n = 4$) ***, $P < 0.001$. (H) SEC14L1 enhances NDV-eGFP replication (top), and SEC14L1 RNAi suppresses NDV-eGFP replication (bottom). HEK293T cells (1×10^5) were transfected with the indicated plasmids. At 24 h after transfection, cells were infected with NDV-eGFP at a multiplicity of infection of 0.001. At 40 h after infection, viral replication was determined by GFP expression visualized by fluorescence microscopy. (I) HEK293T cells were transfected with the indicated plasmids 24 h prior to infection with NDV-eGFP. The percentage of infected cells was determined by flow cytometry analysis of GFP expression. Numbers in parentheses show the detailed percentages of infected cells after transfection with different plasmids.

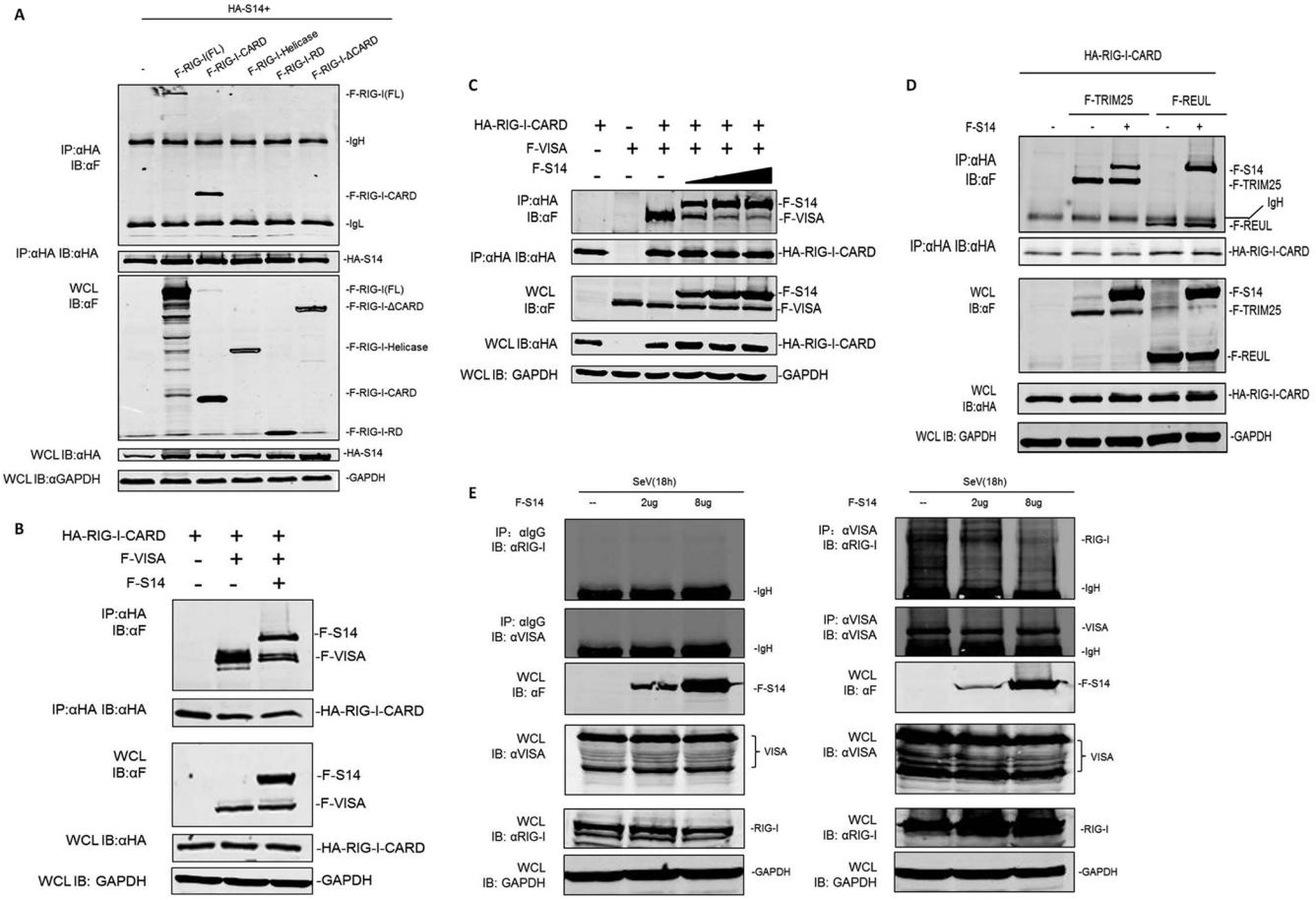

FIG 5 SEC14L1 competes with VISA for RIG-I-CARD binding. (A) SEC14L1 interacts with RIG-I-CARD. HEK293T cells (1×10^6) were transfected with expression plasmids for HA-SEC14L1 alone or together with Flag–RIG-I or its mutants (6 μg each). Cell lysates were immunoprecipitated with anti-HA. The immunoprecipitates were analyzed by Western blotting with anti-HA or anti-Flag antibody. Whole-cell lysates were analyzed by Western blotting with anti-Flag and anti-HA to determine the expression levels of transfected plasmids and with anti-GAPDH as a loading control. (B) SEC14L1 competes with VISA for RIG-I binding. HEK293T cells (1×10^6) were transfected with expression plasmids for HA–RIG-I-CARD alone or together with Flag-VISA or with Flag-VISA and Flag-SEC14L1 (6 μg each). Coimmunoprecipitation was performed as described above for panel A. Whole-cell lysates were analyzed by Western blotting with anti-Flag and anti-HA to determine the expression levels of transfected plasmids and with anti-GAPDH as a loading control. (C) SEC14L1 competes with VISA for RIG-I binding in a dose-dependent manner. HEK293T cells (1×10^6) were transfected with expression plasmids for HA–RIG-I-CARD alone or together with Flag-VISA (6 μg each) and increasing amounts of SEC14L1. Coimmunoprecipitation was performed as described above for panel A. Whole-cell lysates were analyzed by Western blotting with anti-Flag and anti-HA to determine the expression levels of transfected plasmids and with anti-GAPDH as a loading control. (D) SEC14L1 does not compete with TRIM25 and REUL for RIG-I binding. HEK293T cells (1×10^6) were transfected with expression plasmids, as indicated (6 μg each). Coimmunoprecipitation was performed as described above for panel A. Whole-cell lysates were analyzed by Western blotting with anti-Flag and anti-HA to determine the expression levels of transfected plasmids and with anti-GAPDH as a loading control. (E) Overexpression of SEC14L1 abrogates the endogenous interaction between RIG-I and VISA. HEK293T cells (1×10^6) were transfected with expression plasmids for increasing amounts of Flag-SEC14L1 for 18 h and then exposed to SeV for 18 h. Cell lysates were immunoprecipitated with IgG (left) and anti-VISA (right). The immunoprecipitates were analyzed by Western blotting with anti-VISA or anti-RIG-I antibody. Whole-cell lysates were analyzed by Western blotting with anti-Flag, anti-VISA, anti-RIG-I, and anti-GAPDH as a loading control.

bound RIG-I-CARD and suppressed the SeV-triggered activation of IFN-β suggested that SEC14L1 may block RIG-I-CARD signaling to the downstream adaptor. A coimmunoprecipitation analysis was performed to investigate whether SEC14L1 abrogates the interaction between RIG-I-CARD and VISA. HEK293T cells were cotransfected with Flag-VISA and HA–RIG-I-CARD along with Flag-SEC14L1 or an empty vector. SEC14L1 remarkably reduced the interaction between RIG-I-CARD and VISA (Fig. 5B). Increased expression levels of SEC14L1 inhibited the formation of the RIG-I-CARD–VISA complex in a dose-dependent manner. As a control, SEC14L1 had no effect on the interaction between RIG-I-CARD and TRIM25 or REUL (Fig. 5D), which are E3 ligases and known to bind with RIG-I-CARD. Consistently, the endogenous binding between RIG-I and VISA was also dose-dependently reduced by overexpression of SEC14L1 in SeV-infected cells (Fig. 5E).

PRELI-MSF1 and CRAL-TRIO domains of SEC14L1 are required for negative regulation. SEC14L1 contains three domains: the N-terminal-region PRELI-MSF1 domain, the CRAL-TRIO (cellular retinaldehyde and TRIO) domain, and the GOLD domain that is found in SEC14-like proteins (24) (Fig. 6A). To determine which domains are responsible for inhibitory regulation, we made SEC14L1 deletion mutants. Coimmunoprecipitation analysis showed that mutants carrying the first two domains (residues 1 to 300, 301 to 510, and 1 to 510) interacted with RIG-I-CARD, while the mutant carrying the GOLD domain (residues 511 to 719) did not (Fig. 6B). In reporter assays, the

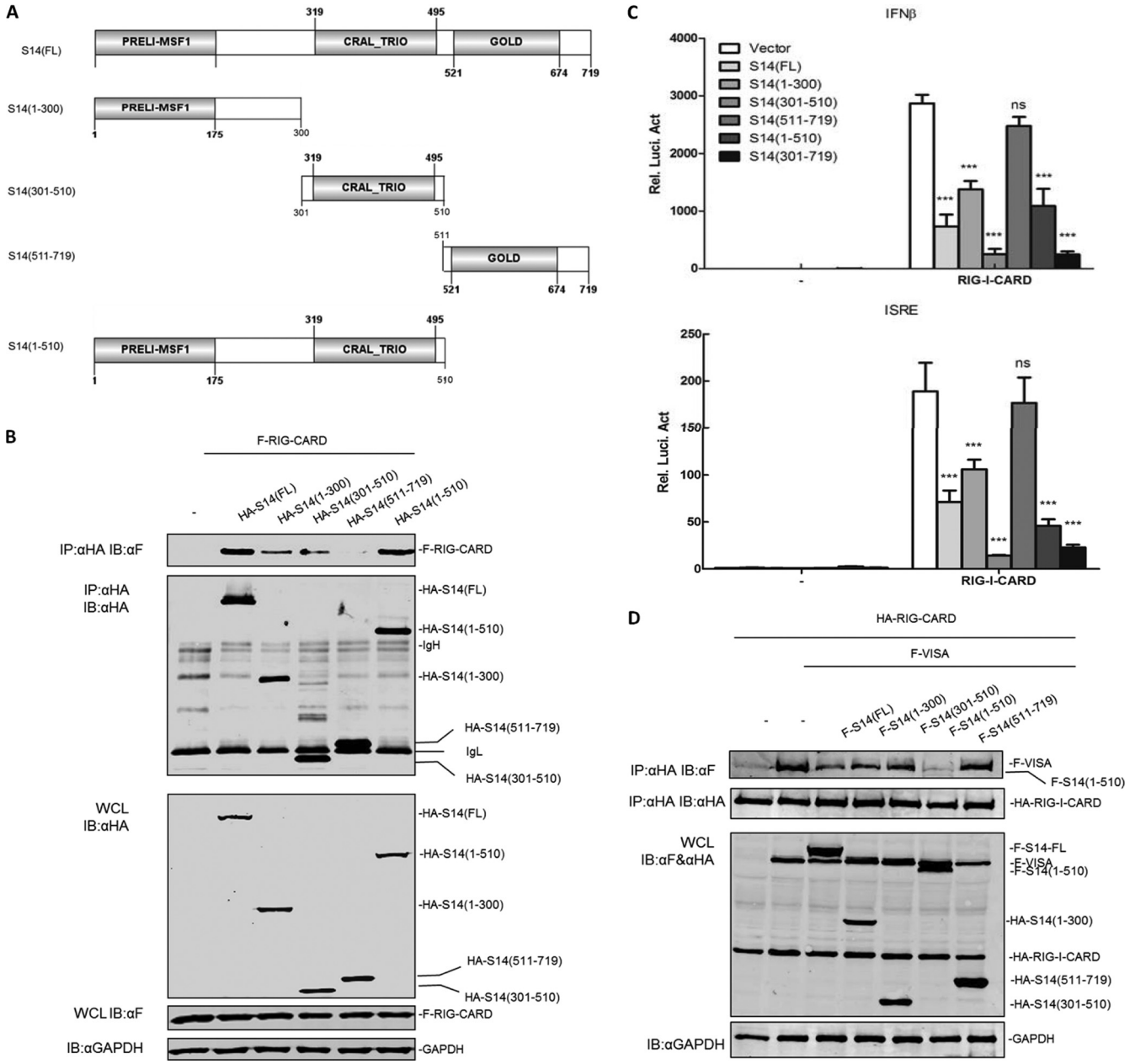

FIG 6 PRELI-MSF1 and CRAL-TRIO domains of SEC14L1 are required for negative regulation. (A) Schematic structures of SEC14L1 and the mutants used in this work. (B) The PRELI-MSF1 and CRAL-TRIO domains of SEC14L1 interact with RIG-I-CARD. HEK293T cells (1×10^6) were transfected with expression plasmids for Flag–RIG-I-CARD alone or together with HA-SEC14L1 and its mutants (6 μg each). Coimmunoprecipitation was performed as described in the legend of Fig. 5A. (C) The PRELI-MSF1 and CRAL-TRIO domains are essential for RIG-I-CARD-induced IFN-β and ISRE promoter activation. HEK293T cells (1×10^5) were transfected with a promoter reporter plasmid (100 ng), the pRL-TK *Renilla* luciferase plasmid (50 ng), and the indicated expression plasmid of SEC14L1 and its mutants (200 ng) along with the empty vector or RIG-I-CARD (100 ng). Reporter assays were performed 24 h after transfection. (D) The PRELI-MSF1 and CRAL-TRIO domains of SEC14L1 but not the GOLD domain compete with VISA for RIG-I binding. HEK293T cells (1×10^6) were transfected with expression plasmids for HA–RIG-I-CARD, Flag-VISA, Flag-SEC14L1, and its mutants (6 μg each), as indicated. Coimmunoprecipitation was performed as described in the legend of Fig. 5A.

mutant carrying the first two domains, PRELI-MSF1 or CRAL-TRIO (residues 1 to 300, 301 to 510, 1 to 510, and 301 to 719), apparently suppressed the RIG-I-CARD-induced IFN-β and ISRE promoters, while the GOLD domain slightly inhibited them (Fig. 6C). In competitive coimmunoprecipitation assays, the SEC14L1 mutant carrying PRELI-MSF1 and CRAL-TRIO inhibited the formation of the RIG-I-CARD–VISA complex, while the GOLD domain did not (Fig. 6D). These data indicate that the PRELI-MSF1 and CRAL-TRIO domains but not the GOLD domain of SEC14L1 are required for the interaction and inhibitory function of SEC14L1.

DISCUSSION

As with other cytokine systems, the production of type I IFN is a transient process and can be hazardous to the host if unregulated, resulting in inflammatory and autoimmune diseases. Various mole-

cules have been shown to regulate the induction of type I IFNs by targeting RIG-I. TRIM25 and REUL/Riplet bind to RIG-I and mediate lysine 63 (K63) ubiquitin ligation, which is critical to the ability of RIG-I to interact with VISA and mediate downstream signaling (15–17), while the E3 ligase ring finger 125 conjugates K48 ubiquitin with RIG-I to promote the proteasomal degradation of RIG-I (30). The deubiquitinase enzyme cylindromatosis and USP17 were shown to mediate the removal of ubiquitin and regulate IFN induction (31, 32). The autophagy conjugate Atg5-Atg12, ISG15, and SUMOylation were reported to inhibit or improve RIG-I signaling (33–35). RIG-I serine 8 phosphorylation induced by protein kinase C α/β (PKC-α/β) and the C-terminal repressor domain (RD) phosphorylated by casein kinase II are also a critical regulatory mechanism (36–38). Recent research has shown that PP1α and PP1γ are the primary phosphatases responsible for RIG-I dephosphorylation and lead to its activation (39).

To identify proteins that can interact with RIG-I and regulate its signaling, we performed a yeast two-hybrid screen using RIG-I as a bait. These efforts led to the identification of REUL (also known as Riplet/RNF135) as an E3 ligase and stimulator of RIG-I (16) and ARF-like protein 16, which inhibits RIG-I by binding with its C-terminal domain in a GTP-dependent manner (40). Here, we report an interaction also uncovered in this screen with SEC14L1, a member of the SEC14-like protein family that may function as a phospholipid transfer protein. Several lines of evidence suggested that SEC14L1 plays a negative role in the RIG-I-mediated pathway. First, endogenous SEC14L1 bound to RIG-I in a viral stimulus-dependent manner, which weakened the RIG-I-mediated antiviral effects. Second, exogenous SEC14L1 reduced the inhibitory effect on viral replication mediated by RIG-I. Third, reduced expression of endogenous SEC14L1 by small interfering RNA (siRNA) and shRNA greatly enhanced the antiviral response. Furthermore, we found that the attenuation of the antiviral effect caused by SEC14L1 was mediated by its interaction with the RIG-I-CARD, which impeded the association between RIG-I and VISA. Notably, the first two domains of SEC14L1 were necessary for its binding to RIG-I and the inhibitory effect. Based on the available evidences, we proposed a functional model of SEC14L1: normally, SEC14L1 does not interact with RIG-I as the autoinhibition structure of RIG-I. Upon viral stimulation, the binding of viral RNA to the C-terminal regulatory domains of RIG-I induces a conformational change, which exposes the CARDs, and SEC14L1 interacts with CARDs and inhibits downstream signaling events.

We confirmed that SEC14L1 specifically interacted with RIG-I, although it also had a weak interaction with VISA (Fig. 1A), which was probably caused by the interaction between overexpressed VISA and endogenous RIG-I. Although in reporter assays, the overexpression of SEC14L1 partly inhibited the VISA-induced IFN-β and ISRE promoters (Fig. 2C), cotransfection of SEC14L1 did not inhibit the VISA-induced mRNA level of IFN-β (Fig. 2D) and the VISA-induced dimerization of IRF3 (Fig. 2E). Most importantly, the endogenous attenuation of SEC14L1 specifically enhanced the activation of the IFN-β and ISRE promoters induced by RIG-I but not VISA, which provided evidences that RIG-I is the major regulatory target of SEC14L1. Even so, we could not exclude the possibility that SEC14L1 also acts on VISA.

The RIG-I-CARD is very important for ubiquitin conjugation, oligomerization, and interaction with VISA to activate downstream IFN-β production. From extensive studies of RIG-I, we now know that ubiquitination of RIG-I is required for activation of the RIG-I-mediated pathway (14). The results shown in Fig. 5D exclude the possibility that SEC14L1 impeded the interaction between RIG-I-CARD and TRIM25 or REUL, the two E3s of RIG-I. Also, SEC14L1 had no effect on the ubiquitination of RIG-I (data not shown). We supposed that SEC14L1 combined with ubiquitinated RIG-I upon SeV stimulation and inhibited the interaction between RIG-I and VISA. Recently, it was shown that disruption of RIG-I oligomerization impairs the ability to activate IRF3 and induce IFN-β (41). We did not determine whether SEC14L1 abolishes the tetramerization of RIG-I. There is a possibility that SEC14L1 and RIG-I-CARD interact with each other and that this abolishes the oligomerization of RIG-I, leading to the inhibitory effect on RIG-I signaling.

SEC14L1 is a poorly characterized member of the SEC14 family in mammals with the potential to control the local phospholipid content in membranes. It has been reported that the interaction of the vesicular acetylcholine transporter and SEC14L1 may affect transporter trafficking (24). Our data suggested a novel innate immune function for SEC14L1. We revealed the inhibitory function of SEC14L1 and the importance of the first two domains, PRELI-MSF1 and CRAL-TRIO, which are less studied than the GOLD domain. The GOLD domain is involved in Golgi function and secretion and interacts with diverse membrane- and lipid-binding proteins. These proteins are predicted to be double-headed adaptors that may help in the assembly of protein complexes on membranes or in the packaging of specific cargo molecules in membranous vesicles (42). In our study, the GOLD domain was not required for the inhibitory effect, did not even interact with RIG-I, and had little effect on reducing the activation of the IFN-β and ISRE promoters induced by RIG-I-CARD (Fig. 6C and D). On the contrary, the PRELI-MSF1 and CRAL-TRIO domains played important roles in associating with RIG-I and inhibitory functions. Recently, it was shown that TAP (α-tocopherol-associated protein) containing the CRAL-TRIO domain protein plays a conserved role in negatively regulating Ras signaling in cancer cell lines (43). We hypothesize that proteins containing the PRELI-MSF1 and CRAL-TRIO domains may also contribute to the regulation of the RIG-I-like receptor signaling pathway. We noticed that the SEC14L1 deletion mutants HA-S14(511-719) and HA-S14(301-510) differ in size by only 1 amino acid, but they exhibit different apparent molecular weights (Fig. 6C and D). We supposed that HA-S14(511-719) was modified, and we plan to analyze it by using mass spectrography.

SEC14L1 is expressed in many types of human cells. We used two cell lines, HEK293T and HT1080, which have high expression levels of SEC14L1, to show an enhanced antiviral response after knockdown of SEC14L1. Both systems led to the same conclusion, further confirming the inhibitory role of SEC14L1 under physiological conditions. We also need to use knockout techniques to further study the physiological significance of SEC14L1 in mice. Although the detailed mechanisms of how RIG-I is inhibited by SEC14L1 need careful structural studies, the identification of a specific inhibitor of RIG-I extends its regulator family and reveals a new function of SEC14L1 in innate immunity.

ACKNOWLEDGMENTS

We thank Li-Ying Du and Xiao-Wei Yan (flow cytometry analyses), Su-Yun Gao (yeast two-hybrid screening), and Xu-Jia Liu (plasmid construction) for technical help.

This work was supported by the National Natural Science Foundation of China (grant 31170822) and the China 973 Program (grant 2010CB911801).

REFERENCES

1. **Kumar H, Kawai T, Akira S.** 2009. Pathogen recognition in the innate immune response. Biochem. J. **420:**1–16.
2. **Takeuchi O, Akira S.** 2010. Pattern recognition receptors and inflammation. Cell **140:**805–820.
3. **Yoneyama M, Kikuchi M, Natsukawa T, Shinobu N, Imaizumi T, Miyagishi M, Taira K, Akira S, Fujita T.** 2004. The RNA helicase RIG-I has an essential function in double-stranded RNA-induced innate antiviral responses. Nat. Immunol. **5:**730–737.
4. **Kato H, Sato S, Yoneyama M, Yamamoto M, Uematsu S, Matsui K, Tsujimura T, Takeda K, Fujita T, Takeuchi O, Akira S.** 2005. Cell type-specific involvement of RIG-I in antiviral response. Immunity **23:** 19–28.
5. **Kato H, Takeuchi O, Sato S, Yoneyama M, Yamamoto M, Matsui K, Uematsu S, Jung A, Kawai T, Ishii KJ, Yamaguchi O, Otsu K, Tsujimura T, Koh CS, Reis e Sousa C, Matsuura Y, Fujita T, Akira S.** 2006. Differential roles of MDA5 and RIG-I helicases in the recognition of RNA viruses. Nature **441:**101–105.
6. **Pichlmair A, Schulz O, Tan CP, Naslund TI, Liljestrom P, Weber F, Reis e Sousa C.** 2006. RIG-I-mediated antiviral responses to single-stranded RNA bearing 5′-phosphates. Science **314:**997–1001.
7. **Hornung V, Ellegast J, Kim S, Brzozka K, Jung A, Kato H, Poeck H, Akira S, Conzelmann KK, Schlee M, Endres S, Hartmann G.** 2006. 5′-Triphosphate RNA is the ligand for RIG-I. Science **314:**994–997.
8. **Yoneyama M, Kikuchi M, Matsumoto K, Imaizumi T, Miyagishi M, Taira K, Foy E, Loo YM, Gale M, Jr, Akira S, Yonehara S, Kato A, Fujita T.** 2005. Shared and unique functions of the DExD/H-box helicases RIG-I, MDA5, and LGP2 in antiviral innate immunity. J. Immunol. **175:** 2851–2858.
9. **Lu C, Xu H, Ranjith-Kumar CT, Brooks MT, Hou TY, Hu F, Herr AB, Strong RK, Kao CC, Li P.** 2010. The structural basis of 5′ triphosphate double-stranded RNA recognition by RIG-I C-terminal domain. Structure **18:**1032–1043.
10. **Kolakofsky D, Kowalinski E, Cusack S.** 2012. A structure-based model of RIG-I activation. RNA **18:**2118–2127.
11. **Saito T, Hirai R, Loo YM, Owen D, Johnson CL, Sinha SC, Akira S, Fujita T, Gale M, Jr.** 2007. Regulation of innate antiviral defenses through a shared repressor domain in RIG-I and LGP2. Proc. Natl. Acad. Sci. U. S. A. **104:**582–587.
12. **Kowalinski E, Lunardi T, McCarthy AA, Louber J, Brunel J, Grigorov B, Gerlier D, Cusack S.** 2011. Structural basis for the activation of innate immune pattern-recognition receptor RIG-I by viral RNA. Cell **147:**423–435.
13. **Cui S, Eisenacher K, Kirchhofer A, Brzozka K, Lammens A, Lammens K, Fujita T, Conzelmann KK, Krug A, Hopfner KP.** 2008. The C-terminal regulatory domain is the RNA 5′-triphosphate sensor of RIG-I. Mol. Cell **29:**169–179.
14. **Zeng W, Sun L, Jiang X, Chen X, Hou F, Adhikari A, Xu M, Chen ZJ.** 2010. Reconstitution of the RIG-I pathway reveals a signaling role of unanchored polyubiquitin chains in innate immunity. Cell **141:**315–330.
15. **Gack MU, Shin YC, Joo CH, Urano T, Liang C, Sun L, Takeuchi O, Akira S, Chen Z, Inoue S, Jung JU.** 2007. TRIM25 RING-finger E3 ubiquitin ligase is essential for RIG-I-mediated antiviral activity. Nature **446:**916–920.
16. **Gao D, Yang YK, Wang RP, Zhou X, Diao FC, Li MD, Zhai ZH, Jiang ZF, Chen DY.** 2009. REUL is a novel E3 ubiquitin ligase and stimulator of retinoic-acid-inducible gene-I. PLoS One **4:**e5760. doi:10.1371/journal.pone.0005760.
17. **Oshiumi H, Matsumoto M, Hatakeyama S, Seya T.** 2009. Riplet/RNF135, a RING finger protein, ubiquitinates RIG-I to promote interferon-beta induction during the early phase of viral infection. J. Biol. Chem. **284:**807–817.
18. **Oshiumi H, Miyashita M, Inoue N, Okabe M, Matsumoto M, Seya T.** 2010. The ubiquitin ligase Riplet is essential for RIG-I-dependent innate immune responses to RNA virus infection. Cell Host Microbe **8:**496–509.
19. **Kawai T, Takahashi K, Sato S, Coban C, Kumar H, Kato H, Ishii KJ, Takeuchi O, Akira S.** 2005. IPS-1, an adaptor triggering RIG-I- and Mda5-mediated type I interferon induction. Nat. Immunol. **6:**981–988.
20. **Meylan E, Curran J, Hofmann K, Moradpour D, Binder M, Bartenschlager R, Tschopp J.** 2005. Cardif is an adaptor protein in the RIG-I antiviral pathway and is targeted by hepatitis C virus. Nature **437:**1167–1172.
21. **Seth RB, Sun L, Ea CK, Chen ZJ.** 2005. Identification and characterization of MAVS, a mitochondrial antiviral signaling protein that activates NF-kappaB and IRF 3. Cell **122:**669–682.
22. **Xu LG, Wang YY, Han KJ, Li LY, Zhai Z, Shu HB.** 2005. VISA is an adapter protein required for virus-triggered IFN-beta signaling. Mol. Cell **19:**727–740.
23. **Hou F, Sun L, Zheng H, Skaug B, Jiang QX, Chen ZJ.** 2011. MAVS forms functional prion-like aggregates to activate and propagate antiviral innate immune response. Cell **146:**448–461.
24. **Ribeiro FM, Ferreira LT, Marion S, Fontes S, Gomez M, Ferguson SS, Prado MA, Prado VF.** 2007. SEC14-like protein 1 interacts with cholinergic transporters. Neurochem. Int. **50:**356–364.
25. **Li X, Xie Z, Bankaitis VA.** 2000. Phosphatidylinositol/phosphatidylcholine transfer proteins in yeast. Biochim. Biophys. Acta **1486:**55–71.
26. **Chinen K, Takahashi E, Nakamura Y.** 1996. Isolation and mapping of a human gene (SEC14L), partially homologous to yeast SEC14, that contains a variable number of tandem repeats (VNTR) site in its 3′ untranslated region. Cytogenet. Cell Genet. **73:**218–223.
27. **Kalikin LM, Bugeaud EM, Palmbos PL, Lyons RH, Jr, Petty EM.** 2001. Genomic characterization of human SEC14L1 splice variants within a 17q25 candidate tumor suppressor gene region and identification of an unrelated embedded expressed sequence tag. Mamm. Genome **12:**925–929.
28. **Lin R, Heylbroeck C, Pitha PM, Hiscott J.** 1998. Virus-dependent phosphorylation of the IRF-3 transcription factor regulates nuclear translocation, transactivation potential, and proteasome-mediated degradation. Mol. Cell. Biol. **18:**2986–2996.
29. **Servant MJ, Grandvaux N, Hiscott J.** 2002. Multiple signaling pathways leading to the activation of interferon regulatory factor 3. Biochem. Pharmacol. **64:**985–992.
30. **Arimoto K, Takahashi H, Hishiki T, Konishi H, Fujita T, Shimotohno K.** 2007. Negative regulation of the RIG-I signaling by the ubiquitin ligase RNF125. Proc. Natl. Acad. Sci. U. S. A. **104:**7500–7505.
31. **Friedman CS, O'Donnell MA, Legarda-Addison D, Ng A, Cardenas WB, Yount JS, Moran TM, Basler CF, Komuro A, Horvath CM, Xavier R, Ting AT.** 2008. The tumour suppressor CYLD is a negative regulator of RIG-I-mediated antiviral response. EMBO Rep. **9:**930–936.
32. **Chen R, Zhang L, Zhong B, Tan B, Liu Y, Shu HB.** 2010. The ubiquitin-specific protease 17 is involved in virus-triggered type I IFN signaling. Cell Res. **20:**802–811.
33. **Jounai N, Takeshita F, Kobiyama K, Sawano A, Miyawaki A, Xin KQ, Ishii KJ, Kawai T, Akira S, Suzuki K, Okuda K.** 2007. The Atg5 Atg12 conjugate associates with innate antiviral immune responses. Proc. Natl. Acad. Sci. U. S. A. **104:**14050–14055.
34. **Kim MJ, Hwang SY, Imaizumi T, Yoo JY.** 2008. Negative feedback regulation of RIG-I-mediated antiviral signaling by interferon-induced ISG15 conjugation. J. Virol. **82:**1474–1483.
35. **Mi Z, Fu J, Xiong Y, Tang H.** 2010. SUMOylation of RIG-I positively regulates the type I interferon signaling. Protein Cell **1**(3):275–283.
36. **Maharaj NP, Wies E, Stoll A, Gack MU.** 2012. Conventional protein kinase C-alpha (PKC-alpha) and PKC-beta negatively regulate RIG-I antiviral signal transduction. J. Virol. **86:**1358–1371.
37. **Nistal-Villan E, Gack MU, Martinez-Delgado G, Maharaj NP, Inn KS, Yang H, Wang R, Aggarwal AK, Jung JU, Garcia-Sastre A.** 2010. Negative role of RIG-I serine 8 phosphorylation in the regulation of interferon-beta production. J. Biol. Chem. **285:**20252–20261.
38. **Sun Z, Ren H, Liu Y, Teeling JL, Gu J.** 2011. Phosphorylation of RIG-I by casein kinase II inhibits its antiviral response. J. Virol. **85:**1036–1047.
39. **Wies E, Wang MK, Maharaj NP, Chen K, Zhou S, Finberg RW, Gack MU.** 2013. Dephosphorylation of the RNA sensors RIG-I and MDA5 by the phosphatase PP1 is essential for innate immune signaling. Immunity **38:**437–449.
40. **Yang YK, Qu H, Gao D, Di W, Chen HW, Guo X, Zhai ZH, Chen DY.** 2011. ARF-like protein 16 (ARL16) inhibits RIG-I by binding with its C-terminal domain in a GTP-dependent manner. J. Biol. Chem. **286:** 10568–10580.
41. **Jiang X, Kinch LN, Brautigam CA, Chen X, Du F, Grishin NV, Chen ZJ.** 2012. Ubiquitin-induced oligomerization of the RNA sensors RIG-I and MDA5 activates antiviral innate immune response. Immunity **36:**959–973.
42. **Anantharaman V, Aravind L.** 2002. The GOLD domain, a novel protein module involved in Golgi function and secretion. Genome Biol. **3:** RESEARCH0023. doi:10.1186/gb-2002-3-5-research0023.
43. **Johnson KG, Kornfeld K.** 2010. The CRAL/TRIO and GOLD domain protein TAP-1 regulates RAF-1 activation. Dev. Biol. **341:**464–471.